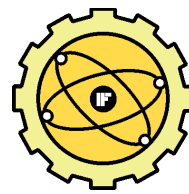




POLSKIE TOWARZYSTWO AKUSTYCZNE



KOMITET AKUSTYKI PAN



INSTYTUT FIZYKI POLITECHNIKI ŚLĄSKIEJ

57. Otwarte Seminarium z Akustyki

Bone ultrasonic scanner

Lucyna CIEŚLIK, Jerzy LITNIEWSKI, Marcin LEWANDOWSKI, Andrzej NOWICKI

Institute of Fundamental Technological Research, Polish Academy of Sciences

Pawińskiego 5B, 02-106 Warszawa

e-mail: lcieslik@ippt.gov.pl

Abstract

Acoustical waves scattered in trabecular bone contain information about its microstructural properties. These properties may change on course of a disease. Standard ultrasonic examinations of bone (densitometry) are performed in transmission and does not provide complete information about bone strength. We have developed the bone ultrasonic scanner that enables measurements of the physical properties of trabecular bone microstructure. Thus the evaluation of bone properties using ultrasonic scanner may be essential for bone diseases diagnosis and treatment monitoring. This study presents application of the scanner operating at 1.5 MHz frequency for examination of trabecular bone (calcaneus) in vivo. Backscattered data were collected and processed in order to obtain power backscattering coefficient (PBSC). Calculated values were compared to these published by several authors in order to verify ultrasonic scanner application as a tool for trabecular bone examination. This study is an approach towards developing a method for the investigation of scattering in trabecular bone that can potentially provide clinically useful information about bone strength and condition.

1. INTRODUCTION

In the last 20 years the quantitative ultrasonic methods were introduced as alternative procedures to radiographic examinations of bone [6, 7, 8]. These methods were based on sound transmission and enabled the determination of the frequency-dependent attenuation coefficient, called BUA (Broadband Ultrasonic Attenuation) and sound velocity – SOS (Speed Of Sound) for the bones that are easily accessible from the outside. Usefulness and applicability of these measurements for prediction of osteoporotic fractures of bones have been proved in long-term studies [4, 19]. Results from many examinations showed that BUA coefficient is closely correlated with BMD (Bone Mineral Density) values, obtained by X-ray densitometry. However, evaluation of bone strength requires not only the knowledge about its density but also about its microstructure.

Ultrasonic examinations of soft tissues, based on the analysis of scattered ultrasonic signal were successfully applied to characterize and to differentiate the tissues [1, 13]. Similarly, signals that have been scattered in trabecular bone contain the information about the properties of the bone structure. Thus, the scattering-based ultrasonic methods potentially enable the assessment of bone microscopic structure.

It has been demonstrated that using the backscattering model it is possible to estimate some microstructural

characteristics from experimental signals measured *in vitro* for calcaneal samples [5, 18]. Many investigations have been focused on the measurements and calculations of the power backscattering coefficient for trabecular bone and the dependency of that coefficient on frequency [2, 9, 10, 17, 20, 21].

In our previous study [12] we have developed a model where thick and thin trabeculae were modeled by two populations of cylindrical scatterers (Fig.1.).

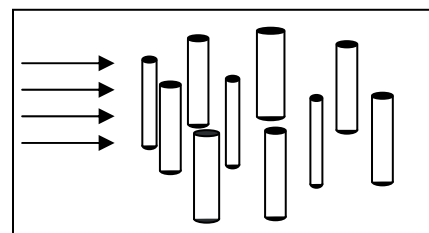


Fig. 1. Trabecular bone model consisting of two populations of cylindrical scatterers. Arrows show the incidence direction of ultrasonic wave

Simulation demonstrated that the physical dimensions, such as size and shape of the individual scatterers, exerted influence on frequency dependence and on the statistics of scattered signals.

It was presented that amplitude histograms calculated using demodulated RF echoes collected using bone ultrasonic scanner deviate from the Rayleigh distribution [3]. These experimental results correspond well with modeling results (model developed by Litniewski et al. [12]) obtained for healthy individuals.

The aim of this study was to perform measurements *in vivo* on calcaneus using ultrasonic bone scanner. Collected data were processed in order to calculate power backscattering coefficient and present the dependence of this coefficient on frequency. Obtained results are compared to the published experimental results [2, 21] in order to verify reliability of ultrasonic bone scanner measurements.

2. MATERIALS AND METHODS

2.1 Trabecular bone structure

There are two types of osseous tissue [15]: trabecular (cancellous) bone (Fig. 2.) and compact bone. Trabecular bone is less dense, softer, weaker, and less stiff in compare to compact bone. The primary structural and functional unit of trabecular bone is the trabecula (Fig. 2. A.) – the tiny lattice-shaped rod or plate. Trabecular bone is highly vascular and contains red or yellow bone marrow (Fig. 2. B.) [15]. Trabecular bone typically occurs at the ends of long bones, proximal to joints and within the interior of vertebrae.

Because of a large surface area of trabeculas of cancellous bone it is characterized by intensive metabolic activity e.g. calcium ions exchange. That is the reason cancellous bone is more severely affected than cortical bone in osteoporosis and other metabolic illnesses of osseous tissue.

Cancellous bone that can be easily examined *in vivo* because of its accessibility is calcaneus (the heel bone).

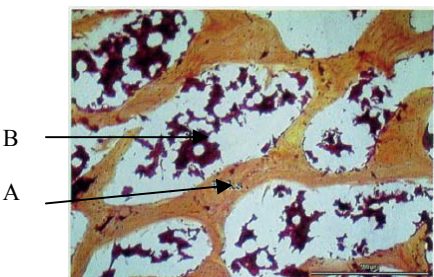


Fig. 2. Histological slide of decalcified trabecular bone (Schmorl stain, zoom 40x). Trabeculae are basic structural units (A) and between them bone marrow (B) is located [14]

2.2 Ultrasonic scanner

Ultrasonic bone scanner (Fig. 4. A.) was developed in our department. The scanner is equipped with single element scanning head with focused (45 mm focal length) spherical transducer (15 mm diameter). It enables transmissions at center frequencies of 1,0 MHz, 1,5 MHz and 1,7 MHz.

The digital programmable coder-digitalizer module based on the field programmable gate array (FPGA) chip supports arbitrary waveform coded transmission and RF echoes sampling up to 20 MHz with 11 bits resolution. FPGA can be easily reprogrammed from the PC at any time. Both the control and data between the PC and the module are passed

via a high-speed USB 2.0 interface. Analog input/output amplifiers, received signal adjustable attenuator and power supply are realized as separate modules for greater modularity and noise immunity. Block diagram (Fig. 3.) of the module reveals its internal architecture.

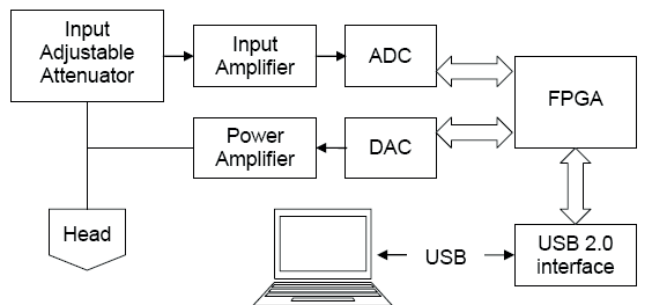


Fig. 3. Block diagram of the coder-digitalizer module

Digital signal processing in our system includes 1D RF signal and 2D image processing. The received sequences were online envelope detected and displayed on the screen. This real-time imaging system provides sector scanning with the image frame rate up to 6 Hz. Chosen data were stored what involved RF data and B-scan (Fig. 4. B.). Since the scanner is equipped with Time Gain Control (TGC), separate file containing these data was stored as well.

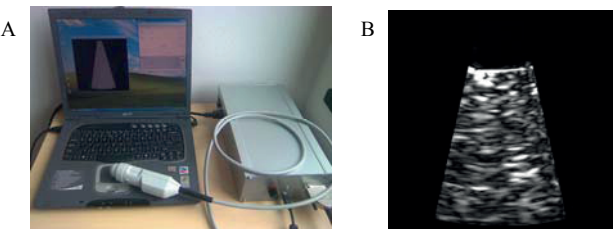


Fig. 4. Ultrasonic bone scanner (A) and exemplary B-scan of trabecular bone *in vivo* (B)

2.3 Data acquisition

In the experiment participated three healthy volunteers (age about 28). The measurements of calcaneus through lateral surface on both legs were performed. The bone was insonified with one period long sinusoidal signals transmitted at driving frequency of 1,5 MHz.

2.4 Signal processing

It is necessary to take into account that there are effects that have impact on signal amplitude and frequency contents. Thus, to obtain reliable results it is necessary to perform adequate operations to neutralize this influence. Signal processing involved compensation of focusing, Time Gain Control (TGC) and attenuation. After signal processing power backscattering coefficient was calculated.

For each particular B-scan the different TGC conditions were applied and stored. Thus, it was possible to obtain gain curve which illustrates the gain level for each sample of echo signal [16]. Next, the respective correction curve that compensated TGC was calculated for each RF data set.

The considered signals were emitted from focused source. Focal distance depends on frequency. Thus it is necessary to compensate this effect before the attenuation

coefficient estimation. In this work the effect of diffraction or focusing was compensated using amplitude spectrum of echoes obtained from a rigid plane reflector located in water perpendicularly to transducer axis at the various axial distances from the source. For each spectral component the correction that compensated the amplitude was calculated. Consequently the attenuation coefficient was then computed using the corrected power spectra.

Attenuation coefficient used to attenuation compensation was obtained for each B-scan separately. The attenuation coefficient $\alpha_0(f)$ was determined using the spectral difference technique based on a comparison of the power spectrum of the backscattered signals recorded before and after propagation through the defined section of the medium. The following procedures were used.

First, selected part of the scattered signal of the duration T was divided into N short partial signals A_i . These signals were separated by the distance Δt [11]:

$$\Delta t = \frac{T - t_0}{N}, \quad (1)$$

where t_0 is Gaussian window length used for A_i signals determination. This size was equal to 1,5 pulse duration.

Afterwards the spectra of A_i signals $|F(A_i)|$ were calculated by fast Fourier transform and partial attenuation coefficients $\alpha_i(f)$ were determined from the formula [11]:

$$\alpha_i(f) = \frac{-\ln\left(\frac{|F(A_{i+1})|}{|F(A_i)|}\right)}{\Delta t \cdot v}, \quad (2)$$

where v is the phase velocity of the longitudinal acoustic wave.

Finally average attenuation coefficient was calculated using following equation:

$$\alpha_0(f) = \frac{1}{N} \sum_N \alpha_i, \quad (3)$$

The following algorithm for the compensation of attenuation was applied. First, the spectrum of attenuated signal FA was calculated. Next, the synthesis of a new signal F on the basis of spectral components of the backscattered signal was performed. During the synthesis, the amplitudes of spectral components were increasing with the increasing value of the depth co-ordinate corresponding to the penetration depth and the value of frequency-dependant attenuation coefficient α_{0k} . The process is described [11] by the formula:

$$F(t_i) = \sum_{k=1}^M FA_k \exp(\alpha_{0k} f_k v t_i) \exp(-2\pi j f_k t_i), \quad (4)$$

where k stands for the index of the spectral component, f_k denotes frequency, FA_k is a complex spectrum of backscattered signal, and α_{0k} is the frequency-dependant attenuation coefficient. $t_i = i \cdot \delta t$ stands for time, where δt is a time step given by the signal sampling rate. The summation

is carried over the whole range of frequencies of backscattered signal. The real part of F is the desired backscattered signal compensated for attenuation.

2.5 Power backscattering coefficient

Power backscattering coefficient was calculated following the equation:

$$PBSC_k = \frac{\langle |F(S)|^2 \rangle_k}{|F(S_0)|^2_k}, \quad (5)$$

where $|F(S)|$ is spatial backscattered power spectrum and $|F(S_0)|$ is reference power spectrum from standard reflecting target. Both signals were recorded in focus zone. k stands for index of spectral component and $\langle \rangle$ denotes spatial averaging operation.

3. RESULTS AND DISCUSSION

Power backscattering coefficient function depends on frequency following power-law function ($PBSC \sim f^n$). PBSC values obtained from *in vivo* experimental measurements were calculated following equation (5) and in the range of frequency from 1,0 to 1,7 MHz power-law function fitting curve was calculated for each B-scan respectively.

Fig. 5. presents exemplary experimental data and power-law fit curve for each volunteer.

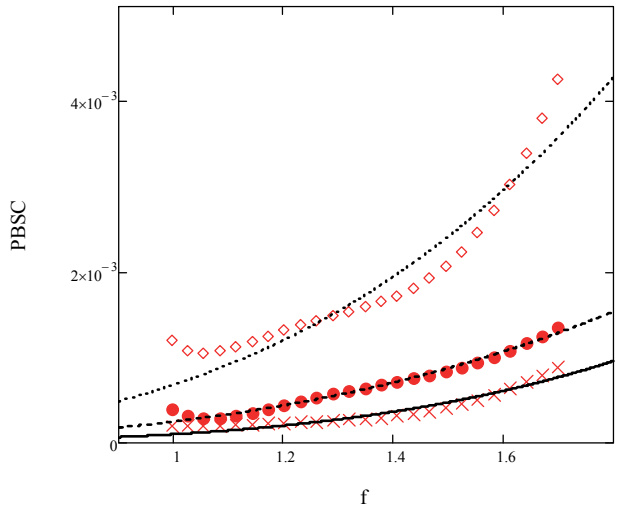


Fig. 5. Power backscattering coefficient $PBSC$ vs. frequency f . Exemplary power-law fit and experimental data for volunteer 1 (dots and dashed line), volunteer 2 (crosses and solid line), volunteer 3 (squares and dotted line)

Fitting curve for volunteer 1 corresponds to exponent value $n = 3,09$ what is minimum obtained result. For volunteer 2 presented curve is for $n = 3,83$ what is maximum calculated result. Exemplary curve for volunteer 3 corresponds to $n = 3,13$.

The frequency dependence of the power backscattering coefficient function obtained from *in vivo* experimental measurements corresponds well with the published experimental results by Chaffai [2] and Wear [21]. Table 1

presents the comparison of the results obtained in these three experiments.

Tab. 1. Results of this study and previously published *in vivo* experimental results

Author	Frequency range [MHz]	Exponent of power-law function
Chaffai et al. [2]	0,3 ÷ 0,7	3,26 ± 0,2
Wear [21]	0,4 ÷ 1,2	3,38 ± 0,3
This study	1,0 ÷ 1,7	3,40 ± 0,3

4. CONCLUSIONS

Obtained exponents of power-law function of *PBSC* correspond to the values published by Chaffai [2] and Wear [21]. This suggests that bone ultrasonic scanner developed in our department gives reliable data and can be applied as a tool for trabecular bone examination. The system may be used both in a laboratory and clinical environment. The high level of system programmability enables implementation of more advanced processing algorithm.

This study is an approach towards developing a tool for the investigation of scattering in trabecular bone that can potentially provide clinically useful information about bone strength and condition.

REFERENCES

1. J. Bamber, C. Hill, J. King, Acoustic properties of normal and cancerous human liver, *Ultrasound in Medicine and Biology*, Vol. 17, 121-133, 1981.
2. S. Chaffai, V. Roberjot, F. Peyrin, G. Berger, P. Laugier, Frequency dependence of ultrasonic backscattering in cancellous bone: Autocorrelation model and experimental results, *Journal of the Acoustical Society of America*, Vol. 108 (5), 2403-2411, 2000.
3. L. Cieślik, J. Litniewski, M. Lewandowski, A. Nowicki, Evaluation of trabecular bone properties using ultrasonic scanner, *Hydroacoustics*, 2010, vol. 13
4. D. Hans, P. Dargent-Moline, A. Schott, J. Sebert, C. Cormier, P. Kotki, et al. Ultrasonographic heel measurements to predict hip fracture in elderly women: the Epidos prospective study, *Lancet*, Vol. 348 (9026), 511-514, 1996.
5. F. Jenson, F. Padilla, P. Laugier, Prediction of frequency-dependent ultrasonic backscatter in cancellous bone using statistical weak scattering model, *Ultrasound in Medicine and Biology*, Vol. 29, 455-64, 2003.
6. C. Langton, The role of ultrasound in the assessment of osteoporosis, *Clinical Rheumatology*, Vol. 13 suppl. 1, 13-17, 1994.
7. P. Laugier, P. Giat, G. Berger, New ultrasonic methods of quantitative assessment of bone status, *European Journal of Ultrasound*, Vol. 1, 23-38, 1994a.
8. P. Laugier, P. Giat, G. Berger, Bone characterization with ultrasound: state of art and new proposal, *Clinical Rheumatology*, Vol. 13 suppl. 1, 22-32, 1994b
9. P. Laugier, P. Giat, C. Chappard, Ch. Roux, G. Berger, Clinical assessment of the backscatter coefficient in osteoporosis, 1997 *IEEE Ultrasonic Symposium*, 1101-1105, 1997.
10. P. Laugier, F. Padilla, E. Camus, S. Chaffai, C. Chappard, F. Peyrin, M. Talmant, G. Berger, Quantitative ultrasound for Bone Status Assessment, *IEEE Ultrasonic Symposium Proceedings*, Vol. 2, 1341-1350, 2000.
11. J. Litniewski, Wykorzystanie fal ultradźwiękowych do oceny zmian struktury kości gąbczastej, IPPT PAN, 113-117, Warszawa, 2006.
12. J. Litniewski, A. Nowicki and P. A. Lewin, Semi-empirical bone model for determination of trabecular structure properties from backscattered ultrasound, *Ultrasonics*, 49, 505-513, 2009.
13. F. L. Lizzi, M. Ostromogilsky, I. Feleppa, M. Rotke, M. Yaremko, Relationship of ultrasound spectral parameters to features of tissue microstructure, *IEEE Transactions on Ultrasonics, Ferroelectrics, and Frequency Control*, Vol. 33, 319-328, 1986.
14. A. Myśliński, P. Trzonowski, M. Okrój, Z. Dobrzańska, *Atlas histologiczny*, Wydawnictwo Pedagogiczne OPERON, 22, Gdańsk, 2002.
15. A. Myśliński, *Podstawy cytofizjologii i histofizjologii*, AMG, 87-89, Gdańsk, 2007.
16. A. Nowicki, *Wstęp do ultrasonografii, Podstawy fizyczne i instrumentacja*, Medipage, 46-47, Warszawa, 2003.
17. F. Padilla, F. Peyrin, P. Laugier, Prediction of backscattered coefficient in trabecular bones using a numerical model of tree-dimensional microstructure, *Journal of the Acoustical Society of America*, Vol. 113 (2), 1122-1129, 2003.
18. W. Pereira, S. Bridal, A. Coron, P. Laugier, Singular spectrum analysis applied to backscattered ultrasound signals from *in vitro* human cancellous bone specimens, *IEEE Transactions on Ultrasonics, Ferroelectrics, and Frequency Control*, Vol. 51, 302-12, 2004.
19. P. Thomson, J. Taylor, R. Oliver, A. Fisher, Quantitative ultrasound (QUS) of the heel predicts wrist and osteoporosis related fractures in women ages 45-75 years, *Journal of Clinical Densitometry*, Vol. 1, 219-225, 1998.
20. K. Wear, B. Garra, Assessment of bone density using ultrasonic backscatter, *Ultrasound in Medicine and Biology*, Vol. 24 (5), 689-695, 1998.
21. K. Wear, Frequency dependence of ultrasonic backscatter from human trabecular bone: Theory and experiment, *Journal of the Acoustical Society of America*, Vol. 106 (6), 3659-3664, 1999.